

High-Pressure Bridgman Grown CdZnTe for Electro-Optic Applications

A. ZAPPETTINI,^{1,2} L. CERATI,¹ A. MILANI,¹ S.M. PIETRALUNGA,¹ P. BOFFI,¹ and M. MARTINELLI¹

1.—Corecom, via Ampère, 30 20131 Milano, Italy. 2.—e-mail: zappettini@corecom.it

The linear electro-optic response of high pressure Bridgman growth semi-insulating $\text{Cd}_{0.9}\text{Zn}_{0.1}\text{Te}$ bulk samples has been characterized. Measurements have been performed in the third optical window for telecommunications around $\lambda = 1.5 \mu\text{m}$. The dependence of the Pockels figure of merit on the modulation frequency and on the intensity of the optical probe beam is presented and discussed. Despite the residual optical absorption, $\text{Cd}_{0.9}\text{Zn}_{0.1}\text{Te}$ is not affected by photo-generated auto-inhibition of the Pockels effect. This can be attributed to the action of an efficient intragap recombination center. It is, therefore, a suitable basic material for electro-optic switching of near-infrared beams at low frequency and quasi-continuous wave (cw) regimes. The implementation of a $\text{Cd}_{0.9}\text{Zn}_{0.1}\text{Te}$ -based cross-bar switch for optical communication applications is also presented, which reaches -30 dB of extinction ratio and sub millisecond response time.

Key words: Cadmium telluride, telluride-based compounds, Bridgman growth, electro-optic modulators, electro-optic switching

INTRODUCTION

The linear electro-optic Pockels effect is one of the most effective mechanisms for the modulation and processing of optical signals and beams.

Among electro-optic materials, crystals of cubic symmetry are particularly attractive because they are optically isotropic in the absence of an externally applied electric field. Cubic highly resistive semiconductors like III-V GaAs and II-VI CdTe:In have been known for decades as electro-optic intracavity modulators for infrared Q-switched laser sources.¹ A promising electro-optic material must show, at the same time, high Pockels figure of merit and suitable photoconductive behavior. Actually, free charge carriers, photoexcited by the unavoidable absorption of light from the incoming beam, result in a volume space-charge distribution that locally shields the externally applied electric field. This mechanism lowers the effective Pockels effect and may result in its complete inhibition at suitable incident optical intensities. In principle, the higher is the absorption, the stronger is the shielding effect. In the past, this has been also exploited to implement all-optical processing of signals.²⁻⁴ However, when dealing with Pockels modula-

tion, the photo-induced shielding results in auto-inhibition of the electro-optic effect at frequencies lower than the inverse of its characteristic time constant. For this reason, GaAs and indium-doped CdTe are not suitable for low frequency and quasi-continuous wave (cw) electro-optical modulation in the near-infrared and, in particular, in the third window for optical communications around $\lambda = 1.5 \mu\text{m}$.

In this work we present the experimental electro-optic characterization of the II-VI ternary alloy CdZnTe, grown from the melt by the high-pressure Bridgman method. Measurements have been focused to evaluate the Pockels efficiency at $\lambda = 1.5 \mu\text{m}$.

In the next section we describe the material and briefly summarize the theoretical aspects of the electro-optic characterization. In the subsequent section the description of the experimental apparatus and the presentation of the results are given. CdZnTe single crystals have also been used as basic material to implement a 2×2 electro-optic switch, operating on free-space propagating signals, to be considered as an elementary cross-bar building block of larger optical switching matrices. The experimental performances of this device are also described in this section. An explanation of the measurements results in the frame of available theories is given in the final section.

(Received November 21, 2000; accepted March 1, 2001)

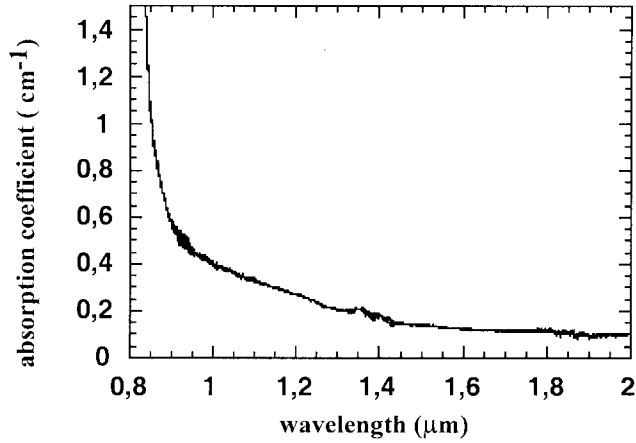


Fig. 1. Optical absorption spectrum of $\text{Cd}_{0.9}\text{Zn}_{0.1}\text{Te}$. A value of $E_g = 1.55$ eV for the bandgap energy can be estimated.

THE MATERIAL

Cubic single crystals of II-VI semiconductor ternary alloy $\text{Cd}_{1-x}\text{Zn}_x\text{Te}$ belong to the zincblende point symmetry group $\bar{4}3m$. We have experimentally characterized the linear electro-optic (EO) response of material with 10% zinc ratio $\text{Cd}_{0.9}\text{Zn}_{0.1}\text{Te}$, working with commercially available samples. The material has been grown from the melt by the high-pressure Bridgman method. This modified version of the vertical Bridgman method enables the production of crystals of large dimensions, high purity, and required semi-insulating characteristics.⁵ The effective performances in terms of Pockels effect are strongly related to the overall optical and electrical features of the semiconductor that still constitute an open field of research.

The optical absorption spectrum of the material under test is shown in Fig. 1. From quantitative reflection and transmission measurements the absorption coefficient at $\lambda = 1.5 \mu\text{m}$ has been evaluated, resulting in $\alpha = 0.23 \text{ cm}^{-1}$. In this spectral range, therefore, the ternary alloy is more absorptive than the binary CdTe:In , for which a value of $\alpha = 0.09 \text{ cm}^{-1}$ has been measured. The nominal 10% zinc content has been confirmed by comparing experimental datum for the absorption edge with the expression for the dependence of the bandgap energy on the alloy composition at room temperature:⁶

$$E_{\text{gap}}(x, 300 \text{ K}) = 1.4637 + 0.49613x + 0.2289x^2 \text{ [eV]} \quad (1)$$

where x represents the zinc fraction.

The dispersion of the refractive index has been modeled using the Sellmeier relation $n^2(\lambda) = A + B\lambda^2/(\lambda^2 - C)$, where interpolation of results by Adachi and Kimura⁷ have been used for the parameters A , B , and C . Values $n_o = 2.736$ and $n_e = 2.732$ are, respectively, derived for binary CdTe and $\text{Cd}_{0.9}\text{Zn}_{0.1}\text{T}$ at $\lambda = 1.55 \mu\text{m}$.

Due to its importance as a basic material for the implementation of x - and γ -ray detectors, the photoconductive and electronic transport properties of CdZnTe have been objects of intense studies in recent

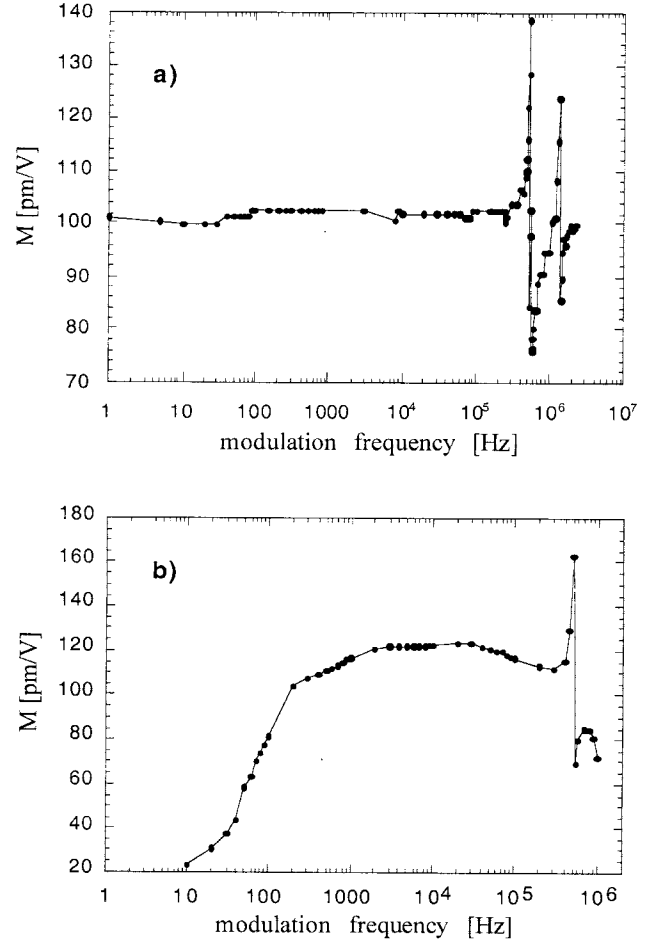


Fig. 2. Spectral dependence of the actual figure of merit for the Pockels effect; (a) undoped $\text{Cd}_{0.9}\text{Zn}_{0.1}\text{Te}$ modulator rod with the dimensions of $2 \times 2 \times 10 \text{ mm}^3$; (b) semi-insulating CdTe:In modulator rod with the dimensions of $2.5 \times 2.5 \times 10 \text{ mm}^3$.

years. In particular, the nature of intragap defect centers in defining the semi-insulating character has been investigated.⁸ Samples tested in the present study were declared to have a resistivity of $10^{11} \Omega\text{cm}$. High resistivity enables the crystals to sustain electric biasing fields with negligible power consumption, which represents a necessary condition for EO modulation.

EXPERIMENTAL RESULTS

The linear EO response of CdZnTe was tested in a Sénarmont compensator-like configuration as detailed in Ref. 9. The probe beam from a semiconductor laser source, tunable between $\lambda = 1460 \text{ nm}$ and $\lambda = 1600 \text{ nm}$, was linearly polarized and collimated in free space propagation to $200 \mu\text{m}$ of waist. The crystal samples were $2 \times 2 \times 10 \text{ mm}^3$ modulators rods, amplitude modulation (AM)-cut, for maximizing EO amplitude modulation effect. A linear polarization analyzer converted the Pockels induced retardation, $\Gamma(t)$, into optical intensity modulation. The transmission at the photodiode followed the well known relation:

$$T = P_{\text{out}}/P_{\text{in}} = \sin^2(\Gamma(t)/2) \quad (2)$$

Table I. Comparison Between Measured Values for Clamped and Unclamped Pockels Coefficients in Cd_{0.9}Zn_{0.1}Te and CdTe:In

Material	$n_0^3 r_{41}$ (pm/V) unclamped	r_{41} (pm/V) unclamped	$n_0^3 r_{41}$ (pm/V) clamped	r_{41} (pm/V) clamped	n_0 ($\lambda = 1550$ nm)
Cd _{0.9} Zn _{0.1} Te	110	5.4	88	4.3	2.732
CdTe:In	110	5.4	82	4.0	2.736

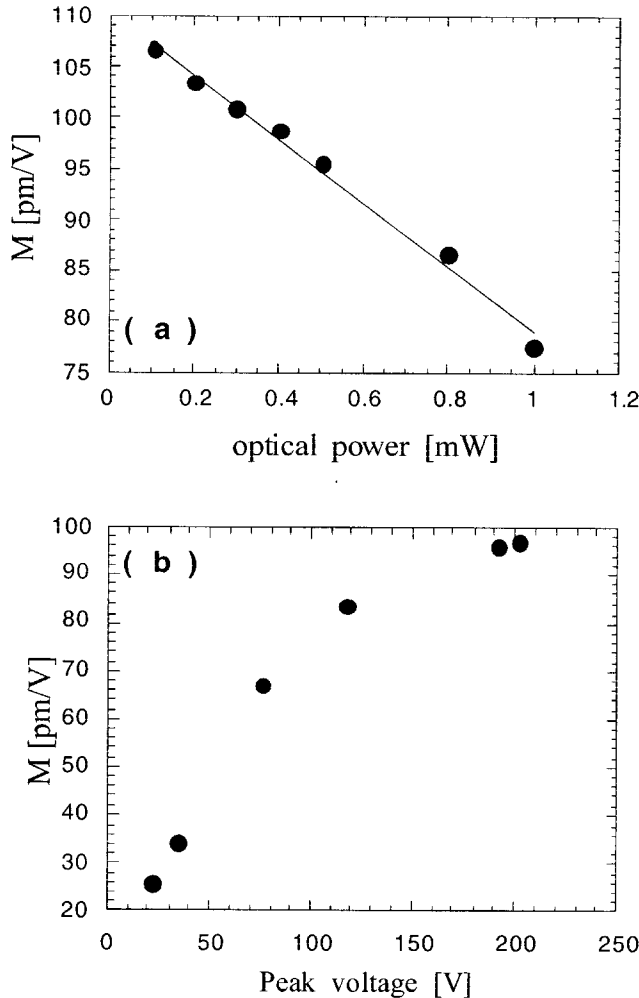


Fig. 3. Characterization of the Pockels figure of merit for Cd_{0.9}Zn_{0.1}Te at f = 1 Hz. (a) dependence on the probe beam intensity; (b) dependence on the peak value of applied voltage V_a . The probe beam power is fixed to $P = 4$ mW.

where $\Gamma(t) = (2\pi/\lambda)(L/d) n_0^3 r_{41} V(t) \Gamma(t)$, λ is the optical wavelength in vacuum, L is the length of the crystal rod, d is the interelectrode spacing, r_{41} is the Pockels coefficient and $V(t)$ is the modulating voltage.

The EO performance of the crystals has been characterized by evaluating the actual figure of merit:

$$M = \left(\frac{\lambda}{2\pi} \right) \left(\frac{d}{L} \right) \cdot \frac{\Delta V_0}{V_0 \Delta V} \Bigg|_{\Delta V \rightarrow 0} \quad (3)$$

where V_0 is the output voltage at the photodiode and ΔV is the peak-to-peak amplitude of the modulating

voltage applied to the crystals. Following its definition, M expresses the Pockels response due to the effective electric field within the volume of the modulator rod, as sensed by the probe beam.

By spanning the modulating frequency from 1 Hz up to 2.2 MHz, M frequency behavior has been obtained, shown in Fig. 2a. In Fig. 2b the analogous result for a semi-insulating CdTe:In rod of $d = 2.5$ mm and $L = 10$ mm is shown. In the high frequency spectral region, the amplitude of M is affected by piezoelectric resonances.¹⁰ As the modulating frequency decreases, M takes on a relatively constant value. In this spectral region, the “unclamped” figure of merit and related EO coefficient, r_{41} , can be determined. At frequencies higher than the first piezoelectric resonance, the “clamped” values can be evaluated. The results for the CdZnTe and CdTe:In samples are reported in Table I.

Both II-VI semiconductors show comparable unclamped and clamped values. However, from comparison of Fig. 2a and b, the superior EO performance of Cd_{0.9}Zn_{0.1}Te becomes evident at low modulating frequencies. At $f < 100$ Hz the M value for CdTe:In dramatically decreases. On the contrary, the Pockels performance of the ternary Cd_{0.9}Zn_{0.1}Te does not substantially change. For better characterization of the field shielding effect in the ternary alloy, the dependence of M on the intensity of the optical beam at low modulating frequencies has been measured. Measurements have been performed at 20 V peak voltage. Results at $f = 1$ Hz are shown in Fig. 3a, where a linear interpolation is also indicated. The actual figure of merit decreases with increasing beam power, reaching a 25% reduction at $P_{in} = 1$ mW. The dependence of M on the peak amplitude of the applied voltage, at constant modulating frequency and optical beam intensity, is shown in Fig. 3b at $f = 1$ Hz and $P_{in} = 4$ mW. M increases with applied voltage and tends to saturate to the unclamped Pockels coefficient $n_0^3 r_{41}$. It is interesting to remark that the onset of this saturation region happens at peak voltage values considerably lower than the estimated half-wave voltage, $V_\pi = 1460$ V, of the material, therefore suggesting a good efficiency of modulation on a wide range of retardation values. In particular, EO switching performance of the Cd_{0.9}Zn_{0.1}Te rods has been tested at different optical beam powers. For this, the applied voltage has been switched from $V_a = 0$ V to $V_a = V_\pi = 1460$ V, resulting in a 90° rotation of the linear polarization of the input beam and corresponding on-off intensity modulation after the polarization

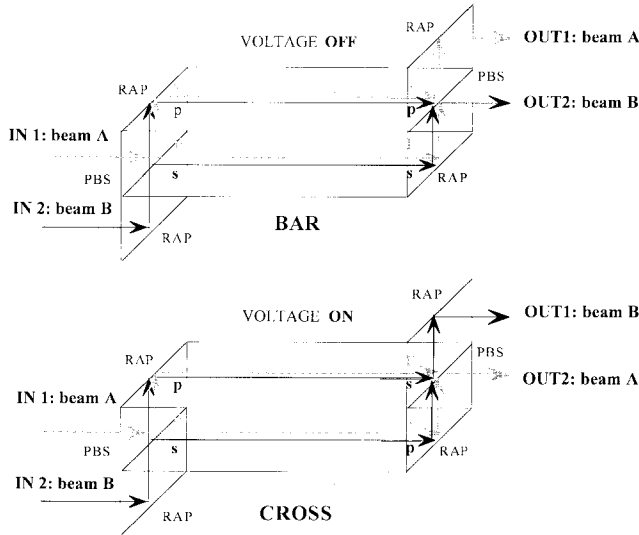


Fig. 4. Schematic representation of the 2×2 $\text{Cd}_{0.9}\text{Zn}_{0.1}\text{Te}$ -based cross-bar switch. (a) In absence of an applied field the switch is in the BAR state. (b) At $V_a = V_\pi$, the crystal acts as a half-waveplate, resulting in spatial switching of the optical beams at the two inputs and CROSS function.

analyzer, following Eq. 2. Increasing the optical power up to $P = 11$ mW did not result in any performance degradation.

A measurement of the dependence of the Pockels effect on probe beam wavelength has also been performed. The wavelength spanned the range from 1480 nm to 1600 nm, and amplitude and frequency of the modulating voltage were kept fixed. Optical power levels lower than $500 \mu\text{W}$ were used. As expected, the value of M remained relatively constant in the wavelength range considered, slightly decreasing in moving to longer wavelengths because of the spectral dependence of the refractive index. This corresponded to a 7% maximum increase in the half-wave voltage.

The polarization switching mechanism has been applied to the implementation of a 2×2 cross-bar switch for optical communication signals. The cross-bar constitutes the elementary building block for more complex architectures of switching matrices, either leading to the optical cross-connect structures or generally to become part of the network node structures, performing circuit switching functions in the optical domain. The scheme of the EO cross-bar elementary switch is shown in Fig. 4. A polarization-diversity architecture has been adopted, so that the performance is independent on the state of polarization (SOP) of the input optical signals. Two polarizing beam splitters (PBS) are used at the input ports to project the SOP of each of the incoming beams on the linear s and p states, at 45° with the EO-induced birefringence axes of the crystal. With the aid of two right-angle prisms (RAP), two separate light paths are produced within the modulator rod, that eventually recombine at the output ports, always using the combination of RAP and PBS. In the absence of external voltage, the linear SOP of the beams within the crystal is unperturbed. This configuration is usu-

ally referred to a "BAR" state, where input ports 1 and 2 are, respectively, connected to output ports 1 and 2. If $V_a = V_\pi$ is applied to the crystal, the linear SOP is 90° rotated, resulting in the exchange of the output port, after recombination. The switching from the bar to the cross state is, therefore, performed. By defining the extinction ratio (ER) between the two channels as the ratio of the input optical power P_{in} to the power P_{out} emerging from the non-connected output, $\text{ER} > 27$ dB for $V_a = V_\pi$ and $\text{ER} = 30$ dB for $V_a = 0$. The insensitivity to the state of polarization of the input signal has been experimentally evaluated to be -30 dB, the limitation being attributed to the polarizing optics and not to the crystal itself. The switching time has also been measured to be less than one millisecond, therefore suitable for circuit switching applications.

DISCUSSION

The experimental tests described above demonstrate that, despite absorption at $\lambda = 1.5 \mu\text{m}$ for undoped $\text{Cd}_{0.9}\text{Zn}_{0.1}\text{Te}$ being stronger than for CdTe:In , the ternary compound exhibits better EO performance. In particular, unclamped and clamped Pockels figure of merit of the two materials can be considered as equivalent, but, as the frequency of the modulating electric field is reduced, the EO effect of CdTe:In is auto-inhibited by a photo-generated local counterfield. On the other hand, the impact of this phenomenon on the ternary alloy can be made negligible.

The role of free-charge carriers in determining the effective local electric field in the bulk of a polarized EO crystal and the related frequency response of the Pockels effect has been object of studies in the past.¹¹ The distribution of optically generated carriers evolves according to the dielectric relaxation time of the material $\tau_d = (\sigma/\epsilon)^{-1}$, where σ is the material conductivity and ϵ the dielectric constant. The EO effect due to spectral components of the externally applied modulating field, which are lower than the dielectric relaxation frequency $\nu = (\sigma/\epsilon)$, is depressed by the reconfiguration of the space charge regions within the volume of the crystal. The electric dipoles associated with the space charge region orient themselves under the influence of the external field, resulting in a shielding of the effective local field. This translates into lowering of the Pockels figure of merit at the considered frequency. The behavior of the field shielding effect at different optical powers of the probe beam can be explained if the following expression for the conductivity is used:⁹

$$\sigma_{\text{TOT}} = \sigma_0(T) + \Delta\sigma(P, T) \quad (4)$$

In Eq. 4, $\sigma_0 = e n \mu_n + e p \mu_p$ and $\Delta\sigma(P) = e \Delta n(P) \mu_n + e \Delta p(P) \mu_p$ are, respectively, the dark value and the photoexcited increase in conductivity, e is the electronic charge, n and p are dark free-carrier concentrations, μ_n and μ_p are mobilities, respectively, for electron and holes. Photo-conductivity can be expressed as:

$$\Delta\sigma(P) = G \tau_c \propto \alpha P \tau_c \quad (5)$$

where G is the photoexcitation rate, τ_c is the effective carrier lifetime, α is the absorption coefficient, and P is the optical power.¹² Experimental results of Figs. 2 and 3 can be explained by using the expression for the relaxation frequency, $\nu = (\sigma/\epsilon)$, together with Eqs. 4 and 5. In general, the higher the photo-conductivity from intragap levels the stronger the shielding effect.⁹ From Eq. 5, this corresponds to increasing the beam power and optical absorption. In principle, one could expect the auto-inhibition in $\text{Cd}_{0.9}\text{Zn}_{0.1}\text{Te}$ at $\lambda = 1.5 \mu\text{m}$ to be stronger than in CdTe:In , due to higher absorption coefficient. Actually, the opposite occurs. This can be explained, by taking into account the role of the carrier recombination time, τ_c . This, in turn, is affected by the concentration and nature of the intragap defect centers. In particular, the different shielding effects in the two materials can be explained by admitting τ_c in $\text{Cd}_{0.9}\text{Zn}_{0.1}\text{Te}$ to be reduced by the presence of a fast recombination center.^{4,13} Nevertheless, at quasi-cw regimes the penalty in Pockels figure of merit becomes considerable, as shown in Fig. 2a, and worsen with beam power. However, as shown in Fig. 2b, by increasing the modulating peak voltage, the effect of the counter-field is progressively reduced, until M eventually saturates at the nominal unclamped value $n_0^3 r_{41}$. The saturating voltage is lower than V_π , so that full Pockels yield can be reached when operating the modulator as a half-waveplate, even at low frequency regimes and high photoexcitation values. The phenomenon can be explained by admitting that, as the applied electric field is increased, the carrier drift time is reduced and charge collection at the electrodes becomes more effective, resulting in depleting of space charge regions and lowering of the shielding effect.⁹

CONCLUSION

Semi-insulating high-pressure Bridgman growth $\text{Cd}_{0.9}\text{Zn}_{0.1}\text{Te}$ bulk crystals have proven to be a reliable basic materials to perform EO processing of signal beams in the near-infrared range typical of optical communications. In particular, $\text{Cd}_{0.9}\text{Zn}_{0.1}\text{Te}$ -based switches show constant performance on the whole third communication window around $\lambda = 1.5 \mu\text{m}$, both at high and low modulating frequencies. The auto-

inhibition effect, due to the photo-generation of carriers consequent to near-infrared absorption, is reduced with respect to the binary CdTe:In resulting in lower actual half-wave voltage at low modulating frequencies. For these reasons, the ternary alloy is particularly suitable for implementing EO devices to be used as basic building blocks of spatial switching matrices in optical communication network architectures.

ACKNOWLEDGEMENT

The authors thank Dr. A. Baraldi and Prof. R. Capelletti, both of Istituto Nazionale Fisica della Materia (INFN) and Physics Dept. of University of Parma (Italy), for IR absorption spectrum measurements.

REFERENCES

1. J.E. Kiefer, T.H. Nussmeier, and F.E. Goodwin, *IEEE J. Quant. Electron.* QE-8, 173 (1972).
2. W.H. Steier, J. Kumar, and M. Ziari, *Opt. Lett.* 14, 224 (1989).
3. S.M. Pietralunga, P. Boffi, and M. Martinelli, *J. Nonlin. Opt. Phys. Mater.* 5, 587 (1996).
4. A. Zappettini, L. Cerati, A. Milani, S.M. Pietralunga, and M. Martinelli, *J. Cryst. Growth* 214/215, 866 (2000).
5. E. Raiskin and J.F. Butler, *IEEE Trans. Nucl. Sci.* 35, 81 (1988); F.P. Doty and J. F. Butler, *J. Vac. Sci. Technol. B* 10, 1418 (1992); I. Kikuma, A. Kikuchi, M. Yageta, M. Sekine, and M. Furukoshi, *J. Cryst. Growth* 98, 302 (1989).
6. S.M. Johnson, S. Sen, W. Konkel, and M.H. Kalisher, *J. Vac. Sci. Technol. B* 9, 1897 (1991).
7. S. Adachi and T. Kimura, *Jpn. J. Appl. Phys.* 32, 3866 (1993).
8. W. Stadler, D.M. Hoffmann, H.C. Alt, T. Muschik, B.K. Meyer, E. Weigel, G. Mueller-Vogt, M. Salk, E. Rupp, and K.W. Benz, *Phys. Rev. B* 51, 10619 (1995); A. Castaldini, A. Cavallini, B. Fraboni, L. Polenta, P. Fernandez, and J. Piqueras, *Phys. Rev. B* 54, 7622 (1996); C. Szeles, Y.Y. Shan, K.G. Lynn, and E.E. Eissler, *Nucl. Instr. Meth. Phys. Res. A* 380, 148, (1996).
9. A. Milani, E. Bocchi, A. Zappettini, S.M. Pietralunga, and M. Martinelli, *J. Cryst. Growth* 214/215, 913 (2000).
10. A.M. Bogomolov, L.N. Magdich, and V.N. Shmyglya, *Sov. J. Quant. Electron.* 3, 125 (1973); Landolt-Bornstein, NS vol. III/17; J.F. Stephany, *J. Opt. Soc. Amer.* 55, 136 (1965); H. Ekstein, *Phys. Rev.* 66, 108 (1944).
11. I.P. Kaminow, *IEEE J. Quant. Electron.* QE-4, 23 (1968).
12. R.H. Bube, *Photoelectronic Properties of Semiconductors* (Cambridge, U.K.: Cambridge University Press, 1992).
13. M. Hage-Ali, J.M. Koebel, P. Siffert, S. Hassan, A. Lusson, R. Triboulet, G. Marracki, A. Zerrai, K. Cherkaoui, R. Adhiri, G. Bremond, O. Kaitasov, and M.O. Ruault, J. Crestou, *J. Cryst. Growth* 184/185, 1313 (1998).